CHINESE JOURNAL OF PHYSICS VOL. 29, NO. 5 OCTOBER 1991

In-Beam Gamma Ray Spectroscopic Study of ^{118}Xe

C. B. Moon, J. C. Kim, J. U. Kwon and B. N. Sung
Department of Physics, Seoul National University, Seoul 151-742, Korea
and
K. Furuno, T. Komatsubara, T. Hosoda, T. Kaneko, S. C. Jeong,
I. Kurniawan and T. Aoki
Institute of Physics, The University of Tsukuba, Tsukuba 305, Japan

(Received June 18, 1991)

High spin states of ^{118}Xe have been investigated by means of y-ray spectroscopy using the ^{92}Mo(^{29}Si, 2pn) at a bombarding energy of 110 MeV. Several new side bands as well as the yrast band were established.

The first band crossings both in the yrast sequence and in the even-spin sequence of the y-band were observed at $\hbar\omega_c$ = 0.39 MeV and $\hbar\omega_c$ = 0.31 MeV respectively. The y-dependent cranked shell model calculation was performed to interpret the band crossing in the y-band.

I. INTRODUCTION

Recently, several investigations have been made on the structure of neutron deficient Xe, Ba and Ce isotopes. These nuclei are in the mass region with $Z \geq 50$ and $50 \leq N \leq 82$, which is one of the best known transitional regions and provide fruitful testing grounds for detailed theoretical descriptions such as the interacting boson model (IBA)[1] and the cranked shell model (CSM)[2]. The latter approach, in particular, has been successful, only when applied to the well deformed nuclei.

More recently, however, y-dependent CSM[3] approach has been made to describe the band structures of y-soft nuclei in the A ~ 150 transitional regions. And it was pointed out by Frauendorf and May[3] that, in the transitional nuclei, the excitation of quasiparticles changes the average static shape of the nucleus and results in stabilizing the nucleus in different deformations.

So far, the level structures of the neutron deficient Xe isotopes have been studied in detail up to ^{120}Xe.[4-10] For the excited states in ^{118}Xe, the yrast band up to (20^+) state[11-13] and a few levels in γ-band[14] have been reported.

In this article, we report our new results of more extensive measurements on ^{118}Xe and discuss the two-quasiparticle band structures in ^{118}Xe in the framework of the y-dependent CSM. A brief account of the present work has been already given elsewhere.[15]

II. EXPERIMENTAL PROCEDURE AND DATA ANALYSIS

The present experiment was performed with the 12 UD tandem Van de Graaff accelerator at the University of Tsukuba. High spin states in ^{118}Xe were populated by means of the ^{92}Mo (^{29}Si, 2pn) reaction using silicon ion beams $^{29}Si^{+9}$ of E_{lab} = 110 MeV. The target was 1 mg/cm thick metallic ^{92}Mo foil enriched to 90 %. In order to stop recoil products, a thick lead backing was made by evaporating on the target.

The y-ray spectra were acquired with four Ge detectors [two HP Ge and two Ge(Li)], whose energy resolutions were 1.9 ~ 2.5 keV (FWHM) at 1332 keV y-ray energy. They were positioned at a distance of 18 cm from the target and at angles of 80°, 150°, 210° and 280° with respect to the beam direction. Lead shields were inserted between Ge detectors in order to suppress the cross talk of y-ray due to Compton scatterings. The standard radioactivity source ^{152}Eu was used for the y-ray energy calibration and relative efficiency measurement of Ge detectors. Additionally, two 20.3 cm diameter x 15.2 cm long NaI(Tl) detectors were placed above and below the target as a sum-energy filter.

The $\gamma\gamma$-coincidence measurements were carried out at the beam energy of 110 MeV. Conventional fast/slow coincidence circuit with a time resolution 20 ns was used. During the course of experiments, the event by event data sets fed by the CAMAC system were transferred and accumulated on the disk memory of the VAX/750 computer. After data taking for a certain period, the data on the disk were transferred to magnetic tapes. A total of 1.96 x 10^8 events were recorded on magnetic tapes. The data analysis was done with aid of a VAX/780 computer.

In the off-line analysis, the data sets were added to a 2048 x 2048 2-dimensional spectrum with careful correction for the gain shifts. The gated spectra were obtained by gating with a narrow slice on one axis (e.g. Eyl axis) and subtracting the Compton backgrounds. Examples of gated spectra are shown in Fig. 1.

The angular distribution measurements were performed at a bombarding energy of 110 MeV and at six angles 75°, 90°, 105°, 125°, 148° and 154° with respect to the beam direction, while the one at 90 served as a monitor.

The angular distribution coefficients A_2/A_0 and A_4/A_0 were obtained by fitting a truncated Legendre polynomials of order 4 to the data and are listed in Table I. Fig. 2 shows χ^2-distributions of some spin hypotheses for the 846 and 1022 keV transitions.

One useful quantity obtained in the present n-coincidence measurement and used to distinguish streched dipoles from quadrupoles is the relative intensity ratio $I\gamma(150°)/I\gamma$ (SO°) normalized to 338 keV transition. They are listed in the third column of Table 1. One can clearly see that quadrupole transitions have the value of ~ 1, while dipole ones about < 0.7.

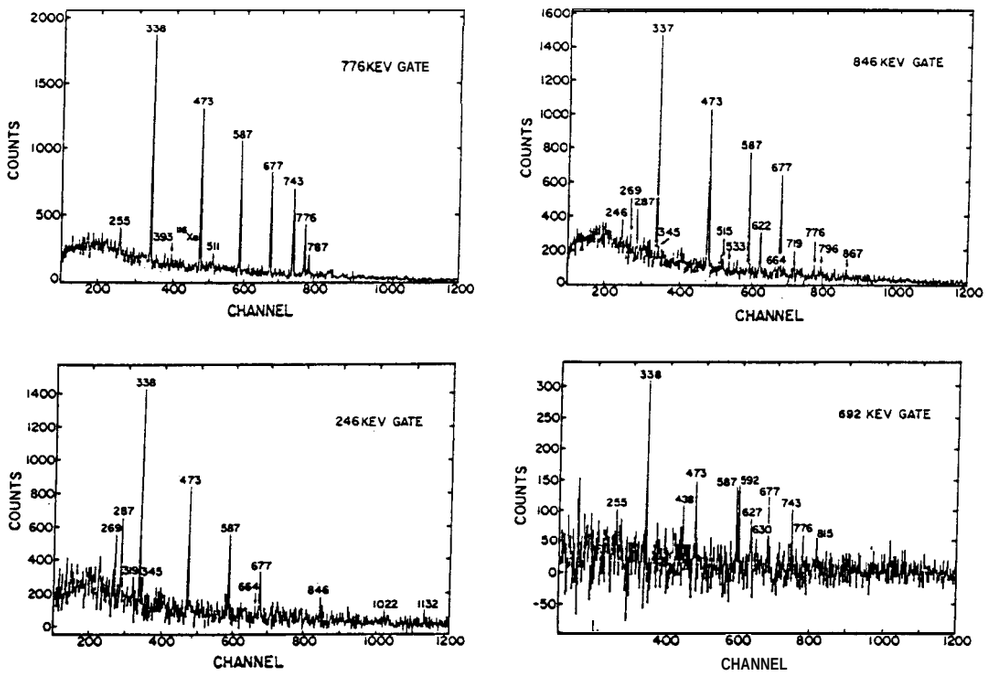

FIG. 1. Coincidence spectra of γ-rays obtained from the ^{92}Mo(^{29}Si, 2pn)^{118}Xe reaction at the incident energy of 110 MeV. Gamma ray energies are labelled in keV.

III. THE LEVEL SCHEME

The y-rays identified in the present work are listed in Table I. The level scheme of ^{118}Xe inferred from our data is shown in Fig. 3. The ordering of levels and spin-parity assignments were based on excitation functions, intensities, y-ray angular distribution and coincidence relations.

The structure in ^{118}Xe was previously studied by Genevey-Rivier et al.[14] and Kerek et al." using the decays of ^{119}Cs and in-beam y-ray spectroscopy respectively.

III-l. The yrast band-band 4

The present level scheme for the ground state band up to the 8^+ state agrees with the previous results of Kerek et al.[11] However, there are several discrepancies in the region above the 8^+ state. Kerek et al. identified the $10^+ \rightarrow 8^+, 12^+ \rightarrow 10^+$ intraband transition y-rays to be 775 keV and 743 keV respectively.

TABLE I. Properties of y-rays assigned to ^{118}Xe in the ^{92}Mo(^{29}Si, 2pn) reaction at E_{lab} = 110 MeV.

$E\gamma$[a](keV)	$I\gamma$[b]	$\frac{I\gamma(156°)}{I\gamma(80°)}$	A_2/A_0	A_4/A_0	$J_i^\pi \rightarrow J_f^\pi$	band labels
191.3	< 1	0.86				2→3262 keV
246.0*	6	0.78				2
254.9	< 1				$(12^+)\rightarrow 12^+$	5→4
274.3	< 1					1→3262 keV
269.0	9	0.80	0.05(17)	-0.05(29)		2
286.9'	15	1.09	0.33(8)	0.02(13)	$(9^-)\rightarrow 9^-$	2→3
319.0*	4	0.79				2
337.7	100	1.00	0.14(1)	-0.05(1)	$2^+\rightarrow 0^+$	4
345.0*	3					2
423.6	1				$7^-\rightarrow 5^-$	3
438.7[c]	10	0.60	0.003(5)	0.27(7)	$(10^+)\rightarrow 10^+$	5→4
438.6'					$(3^+)\rightarrow 2^+$	6→5
457.0	1.5					1
473.1	97	0.94	0.17(1)	-0.05(2)	$4^+\rightarrow 2^+$	4
500.5	9	1.02	0.08(14)	-0.23(25)	$9^-\rightarrow 7^-$	3
513.3[c]*					$4^+\rightarrow 2^+$	5
515.0*	8					2
538.0*		1.18				1
545.0*					$(7^-)\rightarrow 5^-$	1→3
556.5*	7	1.02	0.18(12)	0.02(19)	$6^+\rightarrow 4^+$	5
556.0*					$(5^+)\rightarrow(3^+)$	6
586.9	84	1.00	0.20(2)	-0.07(3)	$6^+\rightarrow 4^+$	4
590.6*	11		0.26(19)	-0.04(31)	$2^+\rightarrow 2^+$	5→4
592.0*		1.11			$(12^+)\rightarrow 10^+$	5
600.4[c]	4	0.81	0.01(8)	0.15(13)	$6^+\rightarrow 6^+$	5→4
622.6'	15	0.97	0.13(8)	-0.11(14)	u--*9-	3
627.6*	6				8+-*6$^+$	5
630.6*	16	0.98	0.81(14)	-0.28(21)	$10^+\rightarrow 8^+$	5
630.8*					$4^+\rightarrow 4^+$	5→4
637.7[c]	8	0.88	0.18(14)	-0.11(26)	$(7^+)\rightarrow(5^+)$	6
637.7[c]						1
664.0*	5	0.77				2
676.9	56	0.95	0.20(2)	-0.02(4)	$8^+\rightarrow 6^+$	4

680.0*					$(9^+)\rightarrow(7^+)$	6
692.3	3	0.84	0.09(28)	-0.33(46)	$(14^+)\rightarrow(12^+)$	5
719.6	7	0.93	0.12(13)	-0.05(20)	$13^-\rightarrow11^-$	3
725.4*	1				$11^-\rightarrow10+$	3→4
737.1[c]	2		0.26(30)	0.01(45)		1
742.9	24	0.93	0.18(6)	0.06(9)	$10^+\rightarrow8^+$	4
775.8	25	0.90	0.16(6)	0.03(10)	$12^+\rightarrow10^+$	4
775.8					$14^+\rightarrow12^+$	4
787.8	3	0.84	0.26(14)	0.51(21)	$16^+\rightarrow14^+$	4
796.6	4	0.94			$(15^-)\rightarrow(13^-)$	3
815.3	1					5
845.7*	21	0.51	-0.09(3)	0.11(4)	$9^-\rightarrow8+$	3→4
847.0*					$(18^+)\rightarrow(16^+)$	4
867.0	2				$(17^-)\rightarrow(15^-)$	3
923.8	2	1.11				1→4
1022.1	14	0.55	-0.13(6)	0.10(10)	$7^-\rightarrow6^+$	3→4
1029.2*	1				$(3^+)\rightarrow(2^+)$	6→4
1103.9	1				$4^+\rightarrow2^+$	5→4
1112.1*	1				$(5^+)\rightarrow(4^+)$	6→4
1132.6	3	0.53	0.13(15)	-0.17(24)	$(9^-)\rightarrow(8^+)$	2→4
1143.5	3	0.47			$(7^-)\rightarrow6^+$	1→4
1162.9	< 1				$(7^-)\rightarrow6+$	6→4
1185.4*	4	0.54	-0.24(26)	0.09(41)	$5^-\rightarrow4^+$	3→4
1187.3*	< 1					3262 keV→4

[a] Uncertainties ± 0.3 keV (*; ± 0.5 keV)

[b] Uncertainties are a few percent for the strong transitions and up to 50 % for the weak.

[c] Contains impurities from another reactions.

Parenthesized numbers in the 4th and 5th column are percentage errors.

In the present work, however, the ordering of the 775 keV and the 743 keV transitions was found to be reversed. The reasons were based on y-ray intensities, excitation functions and, in particular, the relationships to the side bands.

The previously reported" 765 keV ($14^+\rightarrow12^+$) and 812 keV ($18^+\rightarrow16^+$) transitions were not observed in the yrast band. The existence of the 776 keV doublet was evident from the fact that there was a 776 keV line in the spectrum gated by the 776 keV line (see Fig. 1).

Considering the intensities of the 776 and 788 keV γ-rays, we concluded that the second 776 keV line should be placed on top of the 12^+ level. In the spectrum gated on the 847 keV

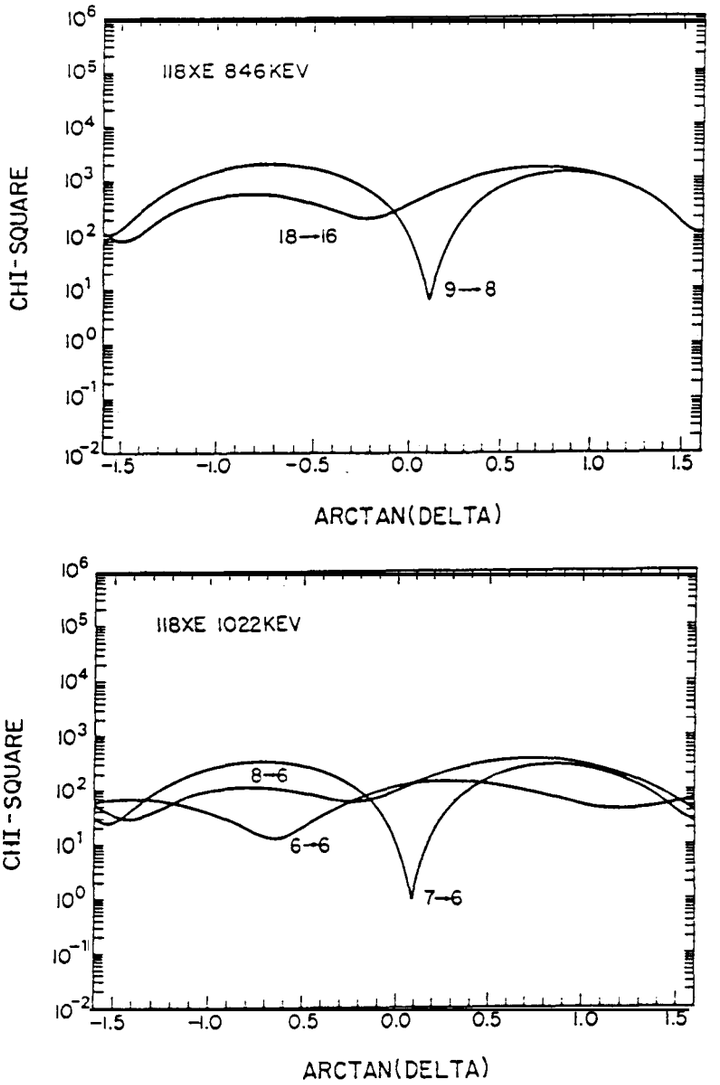

FIG. 2. χ^2-tests for the angular distributions of the 846 keV and 1022 keV transitions in ^{118}Xe.

line, both the 743 keV and the 776 keV peaks were present and the intensities of the 776 keV line was stronger than that of 743 keV. Hence, we assigned the 847 keV line as the $(18^+ \rightarrow 16^+)$ transition. The present yrast level scheme is in a good agreement with the result of Janzen et al.[12]

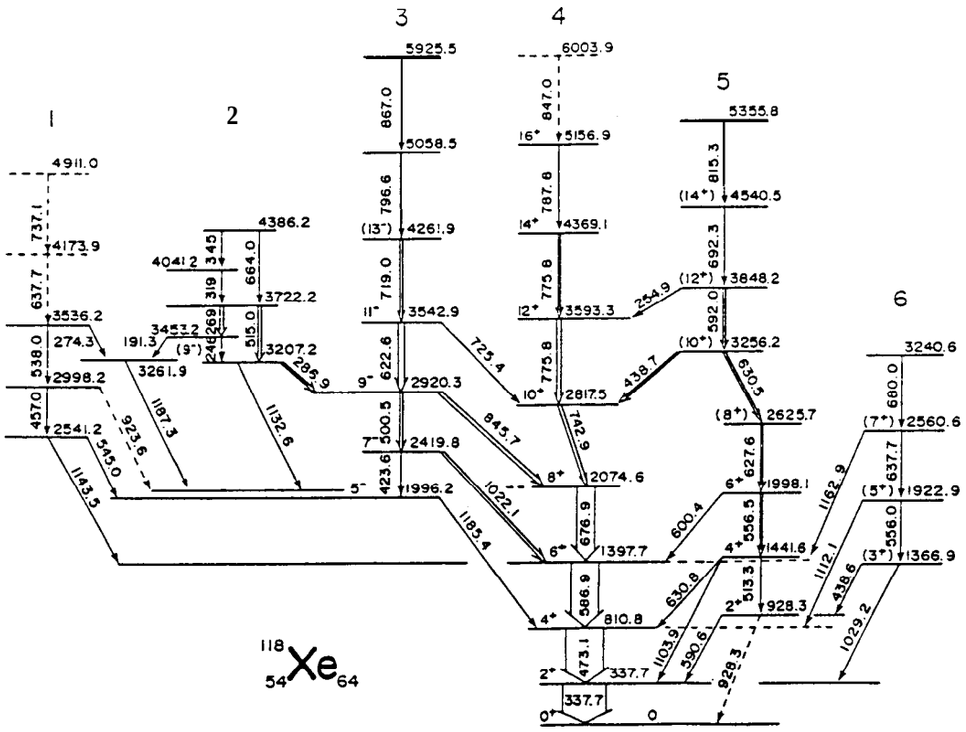

FIG. 3. Level scheme of ^{118}Xe as obtained in the present work. The width of the lines represents their intensity. Weak transitions are drawn in dashed arrows and energies are in keV.

1113. **The negative parity band-band 3**

We began by investigating the **846** keV transition decaying from the 2920 keV level to the ground band 8^+ state. A χ^2-analysis of the angular distribution for the 846 keV y-ray, where as usual a gaussian distribution of magnetic substates was assumed and the mixing ratio δ was varied, showed pure electric dipole characteristics, i.e., 6 = 0 as shown in Fig. 2. Therefore, we have assigned a spin-parity of $J^{\pi} = 7^-$ to the 2920 keV level. There exist similar negative bands in heavier Xe isotopes.[6-10] The 2920 keV state decays also to the 2420 keV level, which in turn feeds into the ground band 6^+ state via the 1022 keV transition. The 1022 keV line showed pure electric dipole nature (see Fig. 2).

We have established the 5^- state at 1996 keV as the band head and it should be noted that $J^{\pi} = 5^-$ band head was not observed in the heavier Xe isotopes.[6-10] The 1996 keV state decays, via the 1185 keV transition, to the ground band 4^+ state and corresponds to the 1994 keV state reported previously by Genevey-Rivier et al.[14]

1113. The gamma band-bands 5 and 6

The quasi y-band built on the 2^+ state at 928 keV confirmed the previous result of ref.[14] up to the 6^+ state at 1998 keV with characteristic strong even-odd staggering. However, the present result extended the even-spin sequence levels up to 5356 keV. The 3256 keV state is remarkable; it decays in approximately equal intensities both to the yrast and to the even y-band level. It should be also remarked, contrary to our expectation, that no transition y-ray from the 12^+ state of band 5 to the 10^+ state of yrast band was observed.

The χ^2-analysis of the 438 keV y-ray indicated mixed transitions of AI = 1 and AI = 2. It, however, contained doublet y-ray from within the y-band and other impurities. Therefore, the spin and parity assignment for this level was tentatively determined by the angular distribution result of the 630 keV intraband y-ray. We would like to point out that no such high spin states in the quasi y-band have been observed in other Xe isotopes so far.

III-4. Bands 1 and 2

The level at the 3207 keV excitation was observed to feed the ground band 8^+ state via the 1133 keV transition. The χ^2-analysis of angular distributions for the 1133 keV line showed both AI = 1 and AI = 2 transition are compatible, giving J^π of the 3207 keV level as 9^- or 10^+. However, the intensity ratio, $I_\gamma(150°)/I_\gamma(80°)$ showed that the 1133 keV transition is more like a dipole character. This band built on the 3207 keV level consists of the AI = 2 cascades interwoven by AI = 1 cascades.

The 2541 keV level decays to the ground band 6^+ state and the negative parity band 5 state by the 1143 keV and 545 keV transitions respectively.. This 2541 keV band head was also observed by Genevey-Rivier et al.[14] The spin-parity of this band head is likely to be 7^- and the band is of the AI = 2 stretch cascade type. However, since its transitions were all very weak, we could neither determine the clear ordering of transition, nor the spin-parity assignments. Finally, the band head at the 3262 keV excitation feeds into the ground band 8^+ state via the 1187 keV transition and is connected to the side bands by the 274 and 192 keV, transitions respectively.

IV. DISCUSSION

IV-l. Experimental and theoretical Routhians

Figure 4a shows the plots of the present experimental Routhians(e') as a function of frequency ω for various bands in ^{118}Xe. The reference was the g-reference, parametrized using the expression:

$$E'_g(\omega) = -\frac{\omega^2}{2}J_0 - \frac{\omega^4}{4}J_1 + \frac{\hbar^2}{8J_0} \qquad (1)$$

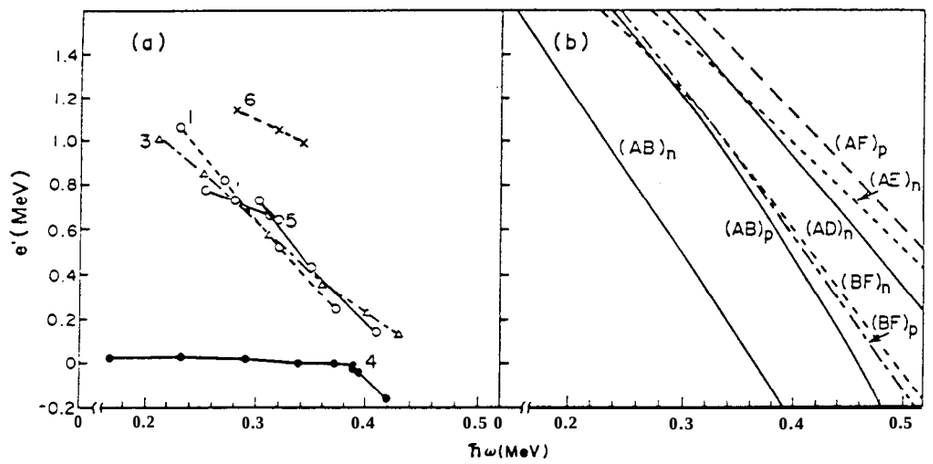

FIG. 4. Part(a) is experimental Routhians(e ') plotted against rotational frequency (hw). The g-reference has been used with parameters $J_0 = 6.3\ MeV^{-1}h^2$ and $J_1 = 110.5\ MeV^{-3}h^4$ as described in the text. Part(b) is theoretical Routhians obtained from CSM calculations in Fig. 5. The quasiparticle notations are same as those in Fig. 5. In (a), the arabic numbers represent the band numbers given in Fig. 3.

where we used the Harris parameters Jo = 6.3 $MeV^{-1}h^2$ and $J_1 = 140.5\ MeV^{-3}h^4$ as determined by fitting the ground state band of ^{118}Xe.

Two backbends are observed in the present experiment, one in the yrast band (band 4) at $h\omega_c = 0.39$ MeV and the other in the y-band (band 5) at $h\omega_c = 0.31$ MeV.

To compare with experimental Routhians, a CSM calculation was performed using the method described by Bengtsson and Frauendorf[2]. Fig. 5 shows the calculated quasiparticle trajectories of ^{118}Xe. For the calculation, we have used the following parameters: quadrupole deformation, $\varepsilon_2 = 0.25$; hexadecapole deformation, $\varepsilon_4 = 0$; triaxiality parameter, $\gamma = -17°$ (the Lund convention); pairing gap parameters for neutrons and protons, An = $\Delta_p = 1.25$ MeV. The value of ε_2 was derived from the B $(E2, 2^+ \rightarrow 0^+)$, which was consistent with the value used in Meyer-ter-Vehn calculation in Xe isotopes.[16] The value of γ was chosen to reproduce the first crossing at $h\omega_c = 0.39$ MeV in the quasineutron trajectories. For the pairing gap parameters, recent compilations of separation energies[17] gave rise to An = 1.37 MeV and $\Delta_p = 1.35$ MeV. However, considering a slight reduction of the pair field in excited configurations*, we chose $\Delta_n = \Delta_p = 1.25$ MeV.

The trajectories A(a), B(b), C(c) and D(d) in Fig. 5 refer to the $h_{11/2}$ orbitals and E(e) and F(f) from the $g_{7/2}$ orbitals, for both quasi-neutrons and protons.

To obtain, in the present CSM calculation, the diabatic trajectories, we incorporated the method developed by Shimizu et al.[18]

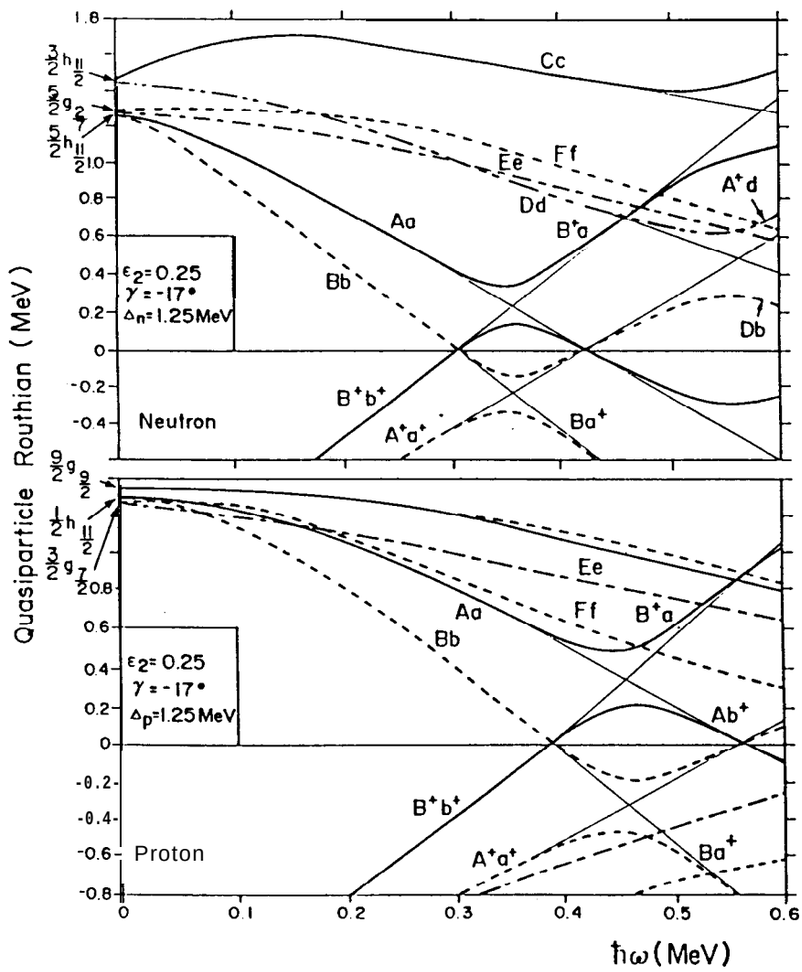

FIG. 5. Cranked shell model calculations for ^{118}Xe. Quasiparticle energies (e') are plotted against rotational frequency ($\hbar\omega$). The full and dash-dotted curves correspond to signature $a = +1/2$ and the dashed and dash-double dotted curves to $a = -1/2$. Diabatic trajectories are labelled with capital letters and adiabatic trajectories with small letters. The trajectories are also labelled at $\hbar\omega = 0$ with their quantum numbers. (a) neutrons; (b) protons.

The theoretical Routhians derived from Fig. 5 in the CSM scheme are presented in Fig. 4b.

In the above CSM calculation, we have assumed the yrast crossing at $\hbar\omega_c = 0.39$ MeV is due to neutron quasiparticles $\nu(h_{11/2})^2$ and adjusted y-deformation as $\gamma = -17°$. In fact, the crossing frequency is very sensitive to the y-value and it was found that withy = $+10°$, the above crossing frequency is also obtainable from the proton quasiparticles $\pi(h_{11/2})^2$.

However, the signature splitting in odd-A neighboring nuclei is also highly sensitive to the y-value. Therefore, we have calculated CSM trajectories for ^{119}Xe (see Fig. 6) using two dif-

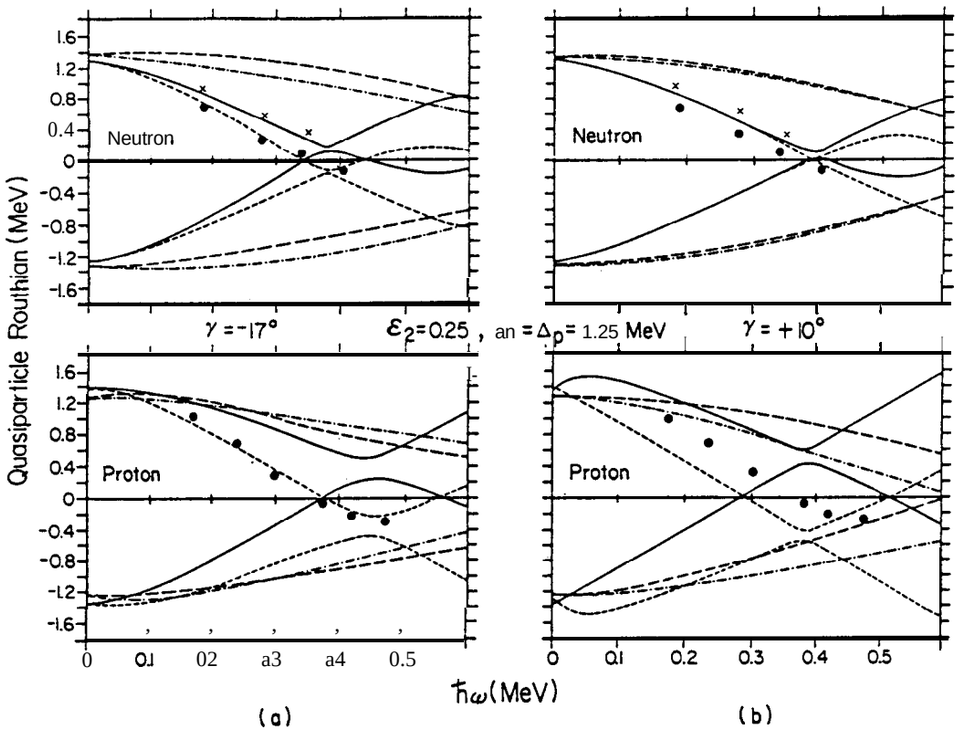

FIG. 6. Cranked shell model calculations for ^{119}Xe. Quasiparticle **energies (e') are plotted against rotational frequency ($\hbar\omega$). The full and short-dashed curves correspond to parity and signature $(-,\pm 1/2)$ and the long-dashed and dot-dashed curves to $(+,\pm 1/2)$. (a) for γ = -17 ; (b) for γ = 10. The experimental data of $\nu h_{11/2}$ for ^{119}Xe are shown by • (a = 1/2) and X (α = -1/2) in quasineutron configurations and $\pi h_{11/2}$ for ^{117}I by • (α = 1/2) in quasiproton configurations. (The odd-even mass differences 1.25 are added in ^{119}Xe and ^{117}I respectively).**

ferent values of y, e.g. -17° and + 10°, and compared with the recent data of ^{119}Xe obtained by Barci et al.[19] The comparison shows that though both neutron and proton quasiparticles predict the backbend near the observed value, the experimental a = $\pm 1/2$ signature splitting of the $h_{11/2}$ quasineutron of ^{119}Xe can not be reconciled with γ = + 10° but with γ = -17°. The unfavored signature levels of ^{117}I [20] have not been observed yet and no comparison could be made. This shows our choice of parameters used in the CSM calculation for ^{118}Xe is consistent with all existing data, and, thereby, the yrast backbend at $\hbar\omega_c$ = 0.39 MeV is probably due to the $\nu(h_{11/2})^2$

alignment, namely $(AB)_n$. This conclusion is corroborated by the fact that the first yrast backbending in ^{122}Xe [8], ^{124,126,128}Xe [21] and ^{130}Xe [4] originates from the same $(AB)_n$.

For the band 3, the comparison with the theoretical Routhians (in Fig. 4b) shows that Routhians are not enough to distinguish $(BF)_p$ from $(BF)_n$. Negative parity bands of a striking similarity to the present, band 3 are also observed in other even zenon isotopes.[6-10]

In ^{120}Xe [9] and ^{124}Xe [7] this band was tentatively interpreted as proton quasiparticle band from blocking argument, though earlier[22] it was ascribed as the configurations of $\nu(h_{11/2}s_{1/2})$ and $\nu(h_{11/2}d_{3/2})$. Recently Hattula et al.[8] observed a backbending of $\nu(h_{11/2})^2$ character in the corresponding negative parity band and concluded the band itself should start as a quasiproton band. Therefore, the band 3 in ^{118}Xe is likely to be $(BF)_p$.

As shown in Fig. 4a, we have observed a backbending in the y-band (band 5) at $\hbar\omega_c$ = 0.31 MeV. Experimental Routhian for the upper section of this y-band are apparently like the $(AB)_p$ configuration in Fig. 4b. However, it is not clear whether one could apply the result of CSM calculation of Fig. 4b, since deformations in the y-band would be considerably different from deformations in the yrast band. To pursue this problem further and also calculate the crossing frequency of the y-band we have employed, in the following section, the y-dependent CSM method recently proposed by Chen et al.[23]

IV-2. Band crossing in the y-band

The y-dependent CSM[3,23] requires to calculate total Routhians E' expressed as a function of rotational frequency ω and γ deformation parameter, i.e.,

$$E'(\omega,\gamma) = \sum_{\mu} e'_{\mu}(\omega,\gamma) + E'_{core}(\omega,\gamma) + e_{\gamma} \tag{2}$$

where e_{μ}', E_{core}' and e_{γ} are the quasiparticle energy, the core energy and the y-vibrational energy respectively. In the above Eq. (2), e_{μ}' are obtained by the standard CSM calculations for the given ω and γ values; E_{core}' has a phenomenological expression[3] as

$$E'_{core}(\omega,\gamma) = \frac{1}{2}V_{po}\cos 3\gamma - \frac{\omega^2}{2}\left(J_0 + \frac{\omega^2}{2}J_1\right)\frac{4}{3}\cos^2(\gamma + 30^\circ) \tag{3}$$

and

$$e_{\gamma} = (E_2+)\frac{9+\sqrt{81-72\sin^2 37}}{9-\sqrt{81-72\sin^2 3\gamma}} \tag{4}$$

where E_2^+ is the excitation energy of the 2^+ state in the ground band. In the present calculation, the prolate-oblate energy difference parameter V_{po} was chosen as V_{po} = -400 keV, which was provided by the signature splitting in the $h_{11/2}$-quasineutron bands of ^{119}Xe nucleus." For

Harris parameters in Eq. (3), $J_0 = 9\ MeV^{-1}h^2$ and Jo = 33 $MeV^{-3}h^4$ were used. These values are obtained from the super band in ^{122}Xe,[8] which is considered more stable. It was found variation of ε_2 parameter within the values of 0.20 ~ 0.25 affected very little the crossing frequency and the signature splitting of the $h_{11/2}$ orbitals in both quasi-neutron and proton. This suggests that the triaxiality parameter γ plays a dominant role.

In the y-dependent CSM calculation, they values of triaxiality are determined as those corresponding to the minimum of total Routhian when they are varied as a function of γ at a given ω value. We have carried out these calculations at $h\omega$ = 0.2, 0.3, 0.4 and 0.5 MeV. Fig. 7 shows a typical result at ho = 0.3 MeV, where total Routhians are plotted as a function of γ.

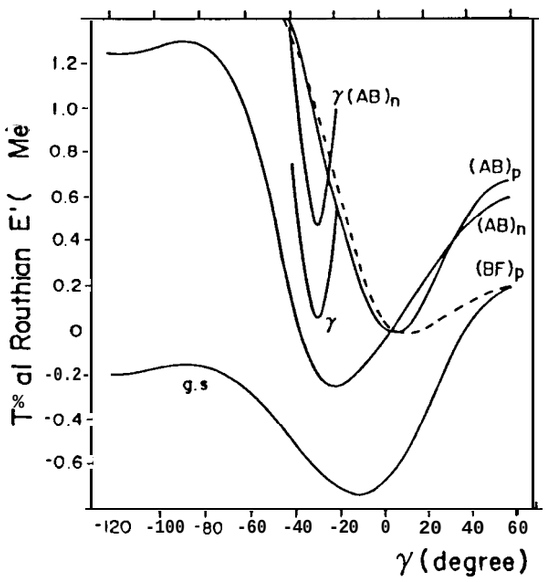

FIG. 7. Total Routhians for the indicated configurations, at $h\omega$ = 0.30 MeV, as function of the triaxiality parameter γ in Lund convention.

Table II lists the γ deformations obtained from these procedures.

Figure 8 shows the plot of total Routhians versus rotational frequency ω as determined by the above y-dependent CSM process.

As shown in Fig. 8, the aligned quasiparticles $(AB)_n$ and $(AB)_p$ predict $h\omega_c$ = 0.27 MeV and 0.30 MeV respectively, both of which are very close to the present experimental result of 0.31 MeV. The $\gamma(AB)_n$ configuration, on the other hand, gives $h\omega_c$ = 0.36 MeV, somewhat larger value. One might prefer $(AB)_n$ to $(AB)_p$ from the fact that the crossing comes earlier and there is a significant transition from the (10^+) state of the band 5 to the 10^+ state of the

TABLE II. They deformation for the various bands in ^{118}Xe obtained by the calculation described in the text.

Band	γ deformations (at $\hbar\omega$ = 0.2, 0.3, 0.4 and 0.5 MeV)			
ground-state	-5°,	-10°,	-15°,	-22°
γ	-30°,	-30°,	-30°,	-30”
$(AB)_n$	-20°,	-20°,	-20°,	-20”
$(AB)_p$	5°,	8°,	5°,	0”
γ $(AB)_n$	-30°,	-30°,	-30°,	-30”
$(BF)_p$*		10”		

* Gamma value represents only at ho = 0.30 MeV.

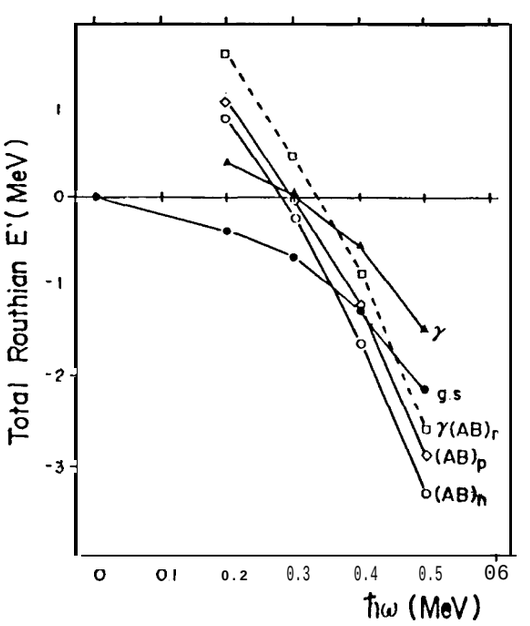

FIG. 8. Calculated total Routhians for ^{118}Xe versus rotational frequency $\hbar\omega$ = 0.2, 0.3, 0.4 and 0.5 MeV. g.s and γ stand for ground state and y-bands. See text for details of quasiparticle configurations.

yrast band. For the case of $(AB)_n$, the lower $\hbar\omega_c$ value compared to that of the yrast band would be explained by the reduction of pairing correlations due to larger y-deformation.

The first backbending in the y-band has been also observed in ^{130}Ce.[24] In their calculation similar to the present, the responsible configuration was attributed to the $\gamma(AB)_p$, while the first backbend in the yrast band was due to the $(AB)_p$ quasiparticles.

ACKNOWLEDGMENT

This work was partly suppolted by the Science Promotion Foundation of Ministry of Education, R.O.K. C.B.M. and J.C.K. would like to express their thanks to the staff of Tandem Accelerator Laboratory of the Tsukuba University for their help and hospitality.

REFERENCES

1. A. Arima and F. Iachello, Phys. Rev. Lett. **35**, 1069 (1975).
2. R. Bengtsson and S. Frauendorf, Nucl. Phys. **A327**, 139 (1979).
3. S. Frauendorf and F. R. May, Phys. Lett. **125B**, 245 (1983).
4. T. Lönnroth, J. Hattula, H. Helppi, S. Juutinen, K. Honkanen and A. Kerek, Nucl. Phys. A431, 256 (1984).
5. T. Lönnroth, S. Vajda, 0. C. Kistner and M. H. Rafailovich, Z. Phys. **A317**, 215 (1984).
6. W. Lieberz, S. Freund, A. Granderath, A. Gelberg, A. Dewald, R. Reinhardt. R. Wiiowski, K. 0. Zell and P. von Brentano, Z. Phys. **A330**, 221 (1988).
7. W. Gast, U. Kaup, H. Hanewinkel, R. Reinhardt, K. Schiffer, K. P. Schmittgen, K. 0. Zell, J. Wrzesinski, A. Gelberg and P. von Brentano, Z. Phys. **A318**, 123 (1984).
8. J. Hattula, S. Juutinen, M. Jääskeläinen, T. Lonnroth, A. Dakkanen, M. Piiparinen and G. Sletten, J. Phys. **G13**, 57 (1987).
9. K. Loewenich, K. 0. Zell, A. Dewald, W. Gast, A. Gelberg, W. Lieberg, P. von Brentano and P. van Isacker, Nucl. Phys. **A460**, 316 (1986).
10. M. S. Rouabah, Th. Byrski, F. A. Beck, D. Curien, B. Hass, J. C. Merdinger, J. P. Vivien, J. Gizon and B. Nyakó, Z. Phys. **A328**, 493 (1987).
11. A. Kerek, T. Lönnroth, K. Honkanen, E. der Mateosian and P. Thieberger, Z. Phys. **A317**, 169 (1984).
12. V. P. Janzen, J. C. Waddington, J. A. Cameron, D. Popescu and D. Rajnauth, McMaster Annual Report (1985) p. 62.
13. V. P. Janzen C. R. Bingham, M. P. Carpenter, L. L. Riedinger, W. Schmitz, J. A. Cameron, J. K. Johansson, D. G. Popescu, D. D. Rajnauth, J. C. Waddington, J. Debug, G. Kajrys, S. Monaro and S. Pilotte, Bull. Am. Phys. Soc. 1096 (1987).
14. J. Genevey-Rivier, A. Char-vet, G. Marguier, C. Richard-Serre, J. D ' auria, A. Huck, G. Klotz, A. Knipper and G. Walter, Nucl. Phys. **A283**, 45 (1977).
15. C. B. Moon, J. C. Kim, T. Komatsubara, T. Kaneko, S. C. Jeong, I. Kurniawan and T. Aoki. Z. Phys. **A331**, 111 (1988).

16. J. Meyer-ter-Vehn, Nucl. Phys. A249, 141 (1975).
17. A. H. Wapstra and G. Audi, Nucl. Phys. A432, 55 (1985).
18. Y. R. Shimizu and K. Matsuyanagi, Prog. Theo. Phys. 74, 1346 (1985).
19. V. Barci, J. Gizon, A. Gizon, J. Crawford, J. Genevey, A. Plochocki and M. A. Cunningham, Nucl. Phys. A383, 309 (1982).
20. W. F.Diel, Jr., P. Chowdhury, U. Garg, M. A. Quader, P. M. Stwertka, S. Vajda and D. B. Fossan, Phys. Rev. C31, 456 (1985).
21. H. El-Samman, V. Barci, A. Gizon, J. Gizon, L. Hildingsson, D. Jerrestan, W. Klamra, R. Kossakowski, Th. Lindblad, T. Bengtsson and G. A. Leander, Nucl. Phys. A427, 397 (1984) and references therein.
22. H. Kusakari, K. Kito, K. Sato, M. Sugawara and H. Katsuragawa, Nucl. Phys. A401, 445 (1983).
23. Y. S. Chen, S. Frauendorf and G. A. Leander, Phys. Rev. C28, 2437 (1983).
24. D. M. Todd, R. Aryaenejad, D.J.G. Love, A. H. Nelson, P. J. Nolan, P. J. Smith and P. J. Twin, J. Phys. G10, 1407 (1984).